

Easy-to-implement hp -adaptivity for non-elliptic goal-oriented problems

Felipe Vinicio Caro Gutiérrez^{2,1}

Supervisors: David Pardo^{1,2,3}, Elisabete Alberdi¹

¹University of the Basque Country (UPV/EHU), Bilbao, Spain

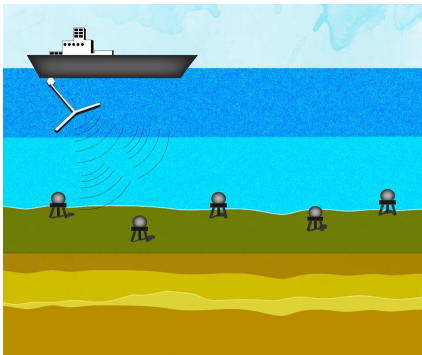
²Basque Center for Applied Mathematics (BCAM), Bilbao, Spain

³Ikerbasque, Bilbao, Spain

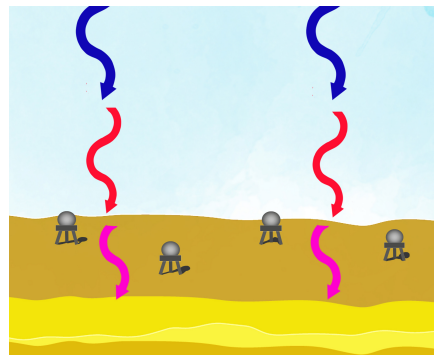
29 November 2023, Leioa



Electromagnetic (EM) Applications



(a) CSEM (artificial source)

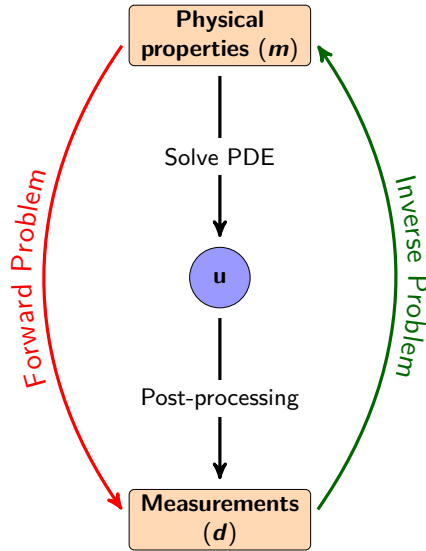


(b) MT (natural source)

Objective

Objective: To obtain the **conductivity/resistivity** distribution of the Earth's subsurface.

Overview of Forward and Inverse Problems



Definitions

\mathcal{F} : Forward Operator
 $m \mapsto d$

\mathcal{I} : Inverse Operator
 $d \mapsto m$

\mathcal{I}_ϕ : Neural Network approximation of \mathcal{I}

Traditional Numerical Methods in Geophysics

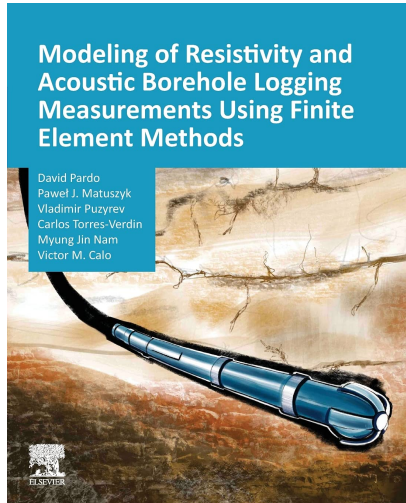


Figure: Published in 2021

Numerical Methods

- Finite Element method
- Finite Difference method
- Finite Volumes method
- Integral methods
- Semi-analytical methods

- ① Goal-Oriented hp -adaptivity for non-parametric PDEs
 - Why hp -adaptivity?
 - Goal-Oriented coarsening strategy
 - 1D Numerical results for Goal-Oriented h - and p -adaptivity
 - 2D Numerical results for hp -adaptivity
- ② Goal-Oriented hp -adaptivity for parametric PDEs.
 - Database generation for DL inversion
- ③ Main Achievements
- ④ Conclusions and Future Work

Goal-Oriented hp -adaptivity for non-parametric PDEs

Why hp -adaptivity?

Advantages

Exponential convergence rates

Local mesh refinement near singularities

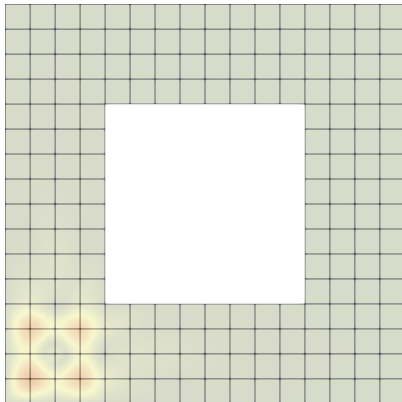
High accuracy per number of degrees of freedom

Limitations

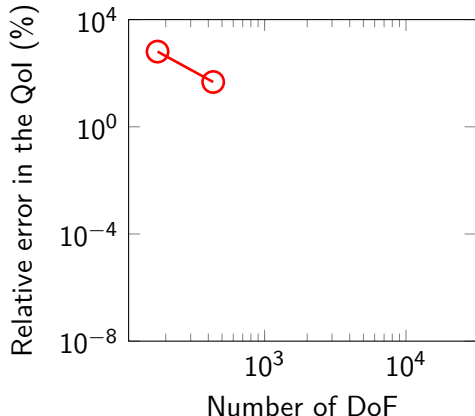
Solution accuracy heavily mesh-dependent, requiring precise mesh design

Large computational costs

Illustrating the Goal-Oriented *hp*-Adaptivity



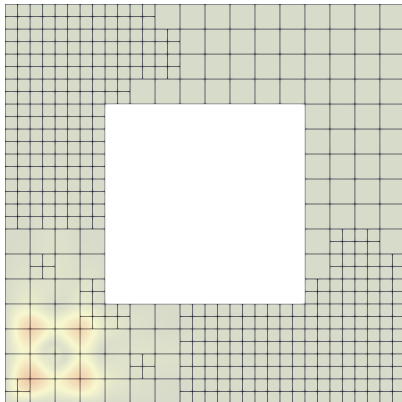
(a) Adaptive iteration 1 of 21



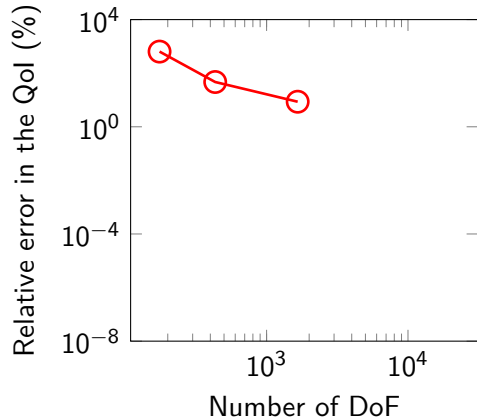
(b) Evolution of the relative error

Figure: Adaptive process for a Helmholtz problem

Illustrating the Goal-Oriented *hp*-Adaptivity



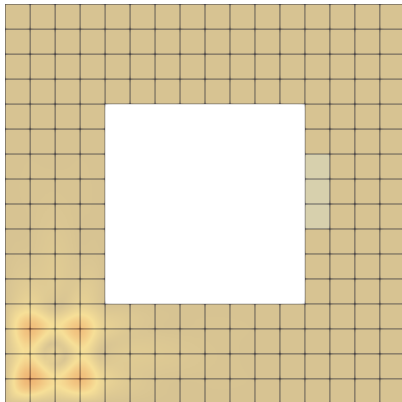
(a) Adaptive iteration 2 of 21



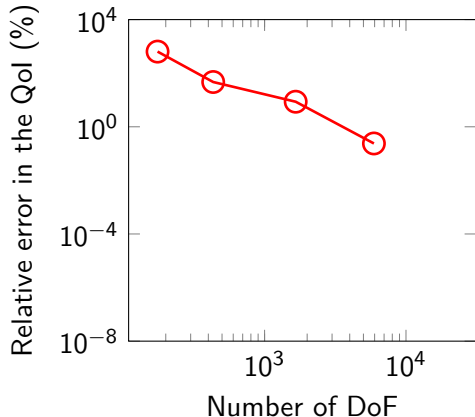
(b) Evolution of the relative error

Figure: Adaptive process for a Helmholtz problem

Illustrating the Goal-Oriented *hp*-Adaptivity



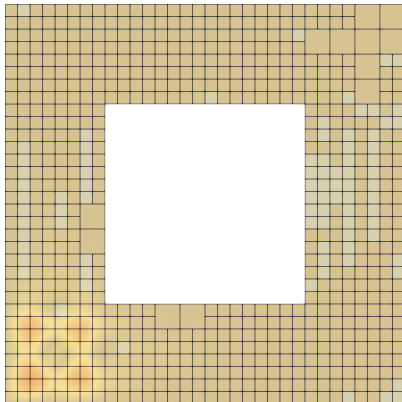
(a) Adaptive iteration 3 of 21



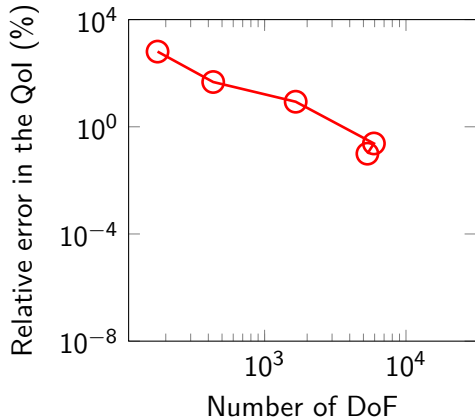
(b) Evolution of the relative error

Figure: Adaptive process for a Helmholtz problem

Illustrating the Goal-Oriented *hp*-Adaptivity



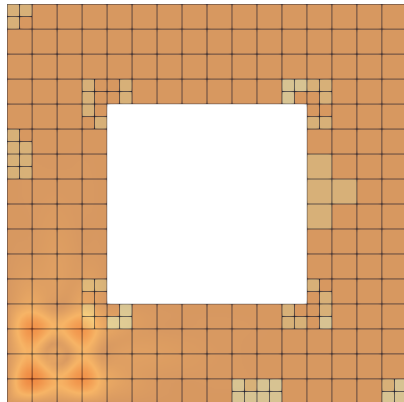
(a) Adaptive iteration 4 of 21



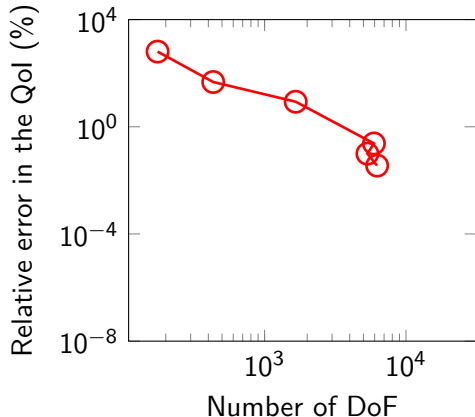
(b) Evolution of the relative error

Figure: Adaptive process for a Helmholtz problem

Illustrating the Goal-Oriented *hp*-Adaptivity



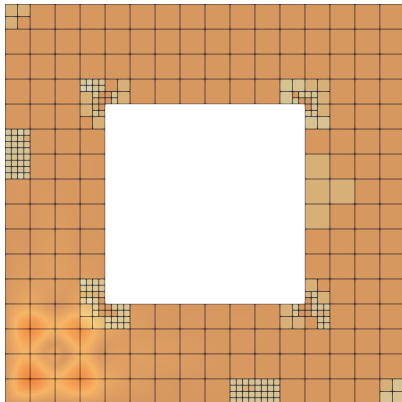
(a) Adaptive iteration 5 of 21



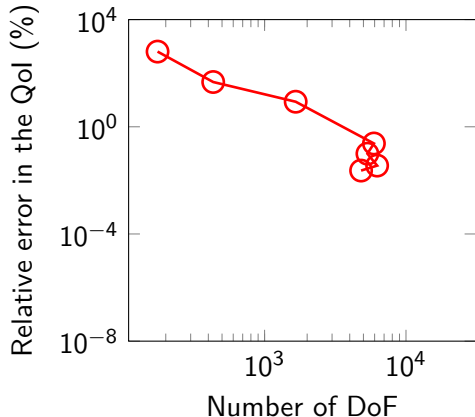
(b) Evolution of the relative error

Figure: Adaptive process for a Helmholtz problem

Illustrating the Goal-Oriented *hp*-Adaptivity



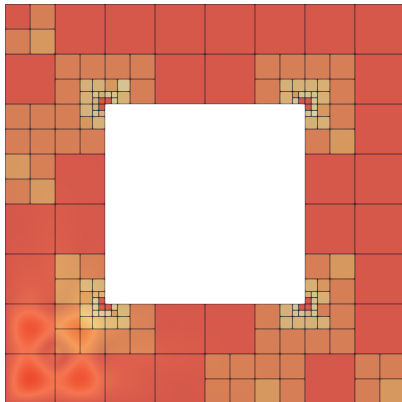
(a) Adaptive iteration 6 of 21



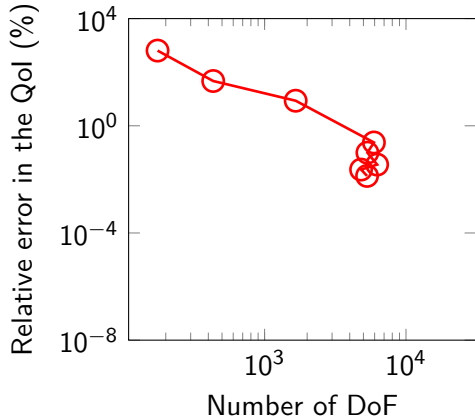
(b) Evolution of the relative error

Figure: Adaptive process for a Helmholtz problem

Illustrating the Goal-Oriented *hp*-Adaptivity



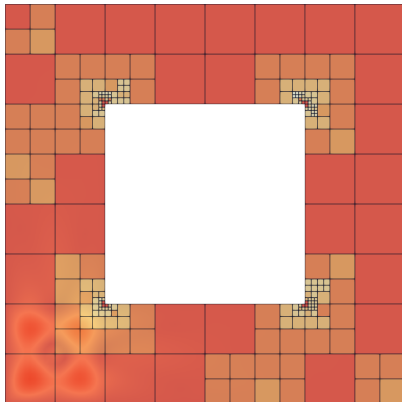
(a) Adaptive iteration 7 of 21



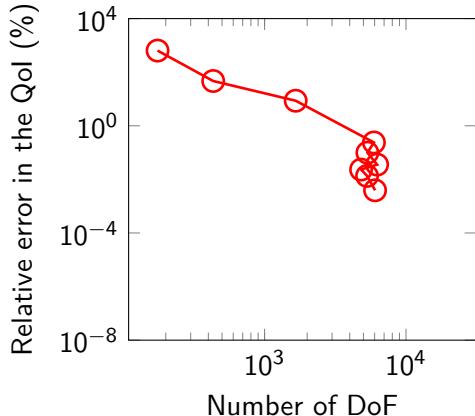
(b) Evolution of the relative error

Figure: Adaptive process for a Helmholtz problem

Illustrating the Goal-Oriented *hp*-Adaptivity



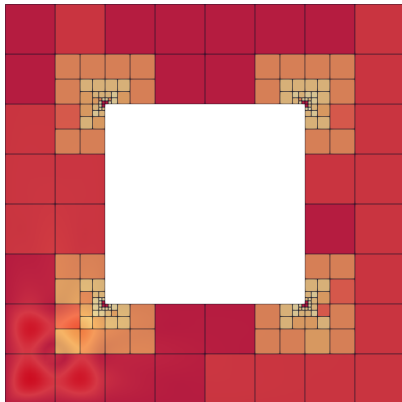
(a) Adaptive iteration 8 of 21



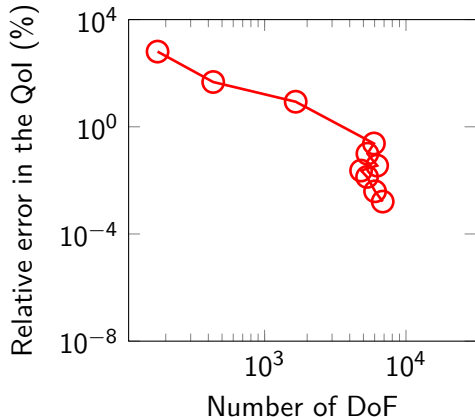
(b) Evolution of the relative error

Figure: Adaptive process for a Helmholtz problem

Illustrating the Goal-Oriented *hp*-Adaptivity



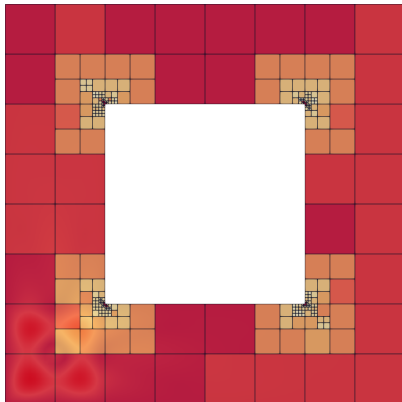
(a) Adaptive iteration 9 of 21



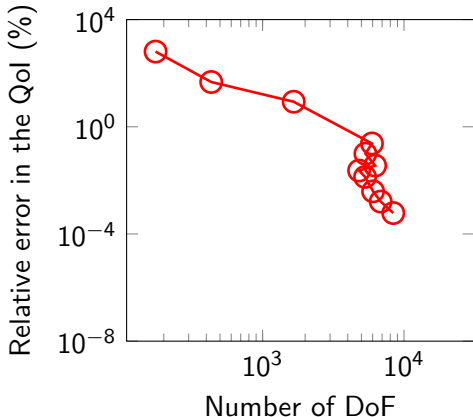
(b) Evolution of the relative error

Figure: Adaptive process for a Helmholtz problem

Illustrating the Goal-Oriented *hp*-Adaptivity



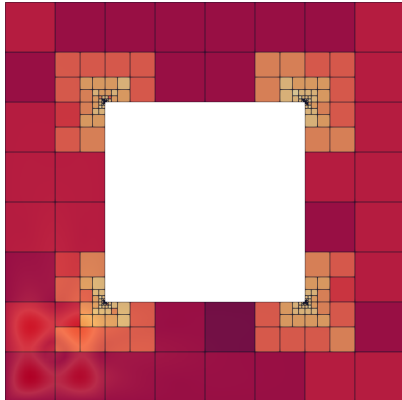
(a) Adaptive iteration 10 of 21



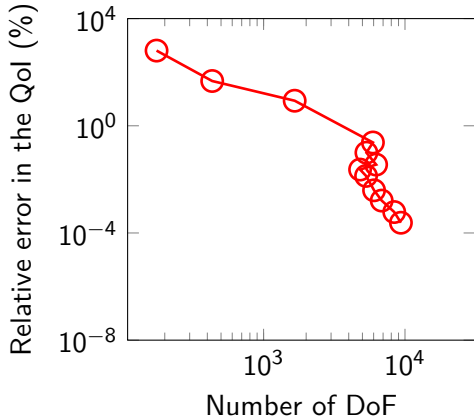
(b) Evolution of the relative error

Figure: Adaptive process for a Helmholtz problem

Illustrating the Goal-Oriented *hp*-Adaptivity



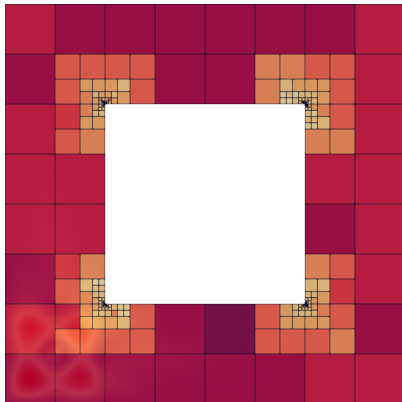
(a) Adaptive iteration 11 of 21



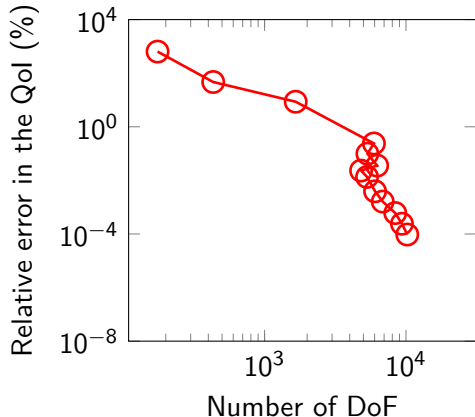
(b) Evolution of the relative error

Figure: Adaptive process for a Helmholtz problem

Illustrating the Goal-Oriented *hp*-Adaptivity



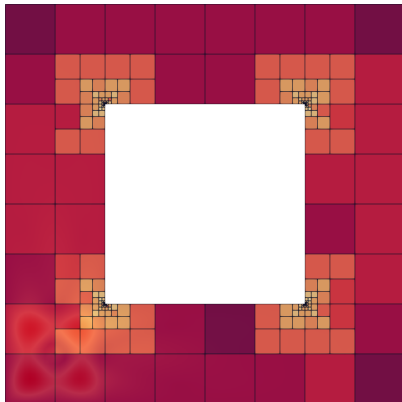
(a) Adaptive iteration 12 of 21



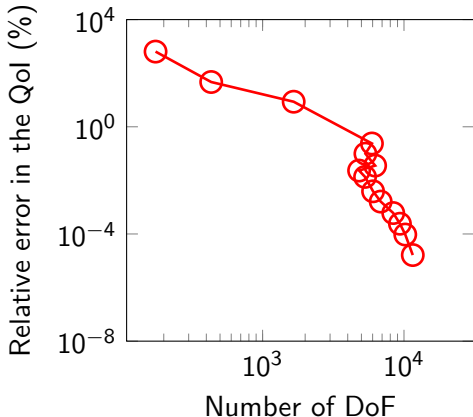
(b) Evolution of the relative error

Figure: Adaptive process for a Helmholtz problem

Illustrating the Goal-Oriented *hp*-Adaptivity



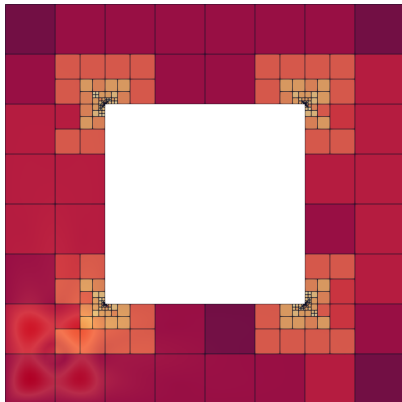
(a) Adaptive iteration 13 of 21



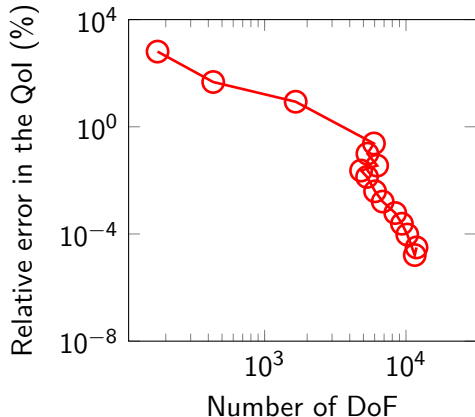
(b) Evolution of the relative error

Figure: Adaptive process for a Helmholtz problem

Illustrating the Goal-Oriented *hp*-Adaptivity



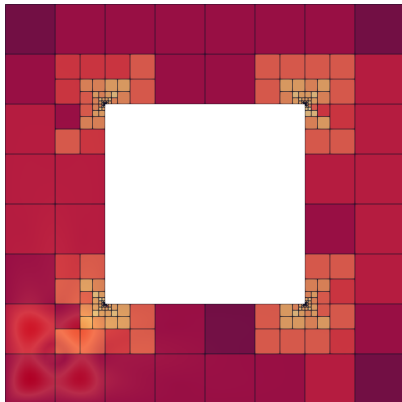
(a) Adaptive iteration 14 of 21



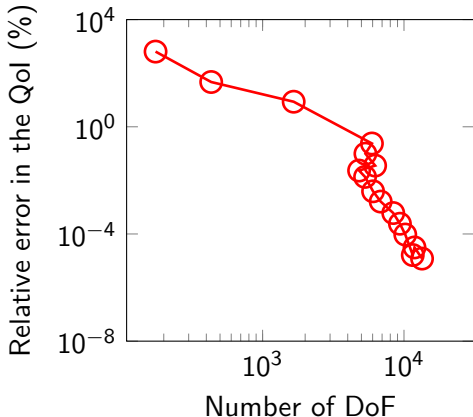
(b) Evolution of the relative error

Figure: Adaptive process for a Helmholtz problem

Illustrating the Goal-Oriented *hp*-Adaptivity



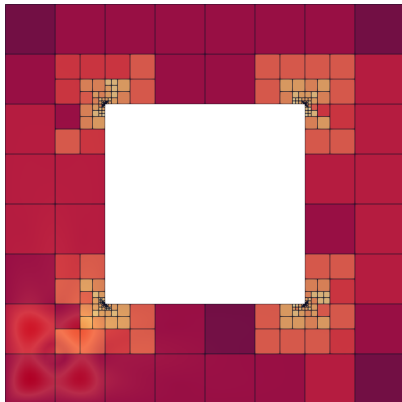
(a) Adaptive iteration 15 of 21



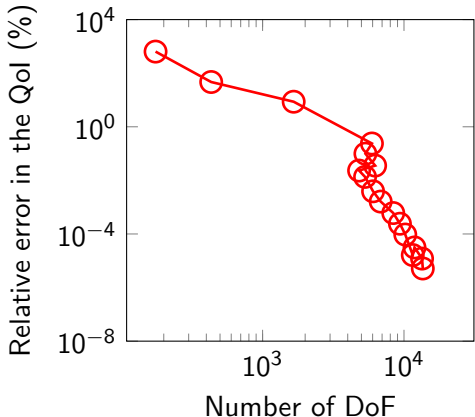
(b) Evolution of the relative error

Figure: Adaptive process for a Helmholtz problem

Illustrating the Goal-Oriented *hp*-Adaptivity



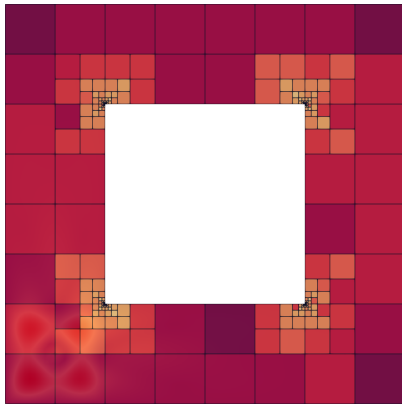
(a) Adaptive iteration 16 of 21



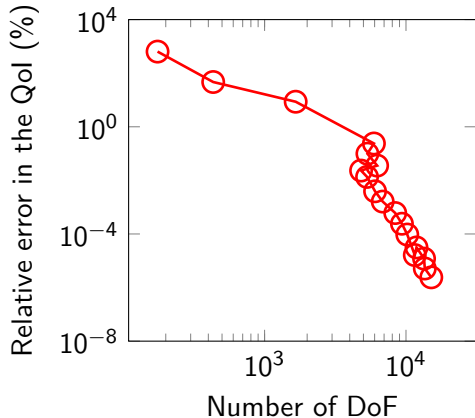
(b) Evolution of the relative error

Figure: Adaptive process for a Helmholtz problem

Illustrating the Goal-Oriented *hp*-Adaptivity



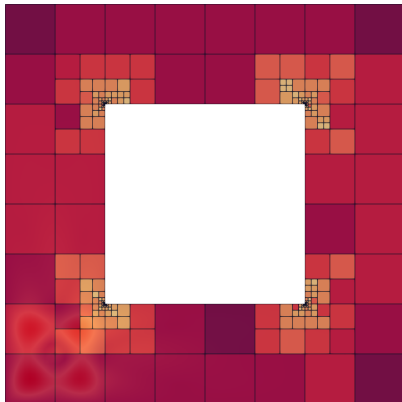
(a) Adaptive iteration 17 of 21



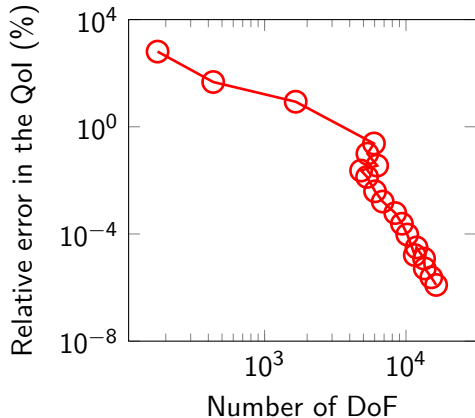
(b) Evolution of the relative error

Figure: Adaptive process for a Helmholtz problem

Illustrating the Goal-Oriented *hp*-Adaptivity



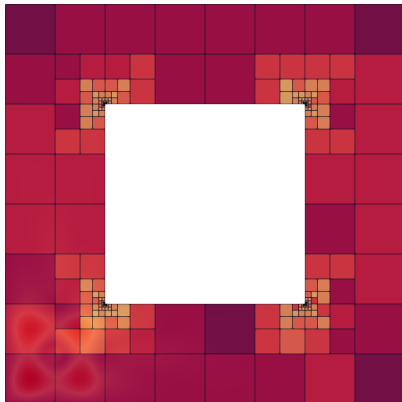
(a) Adaptive iteration 18 of 21



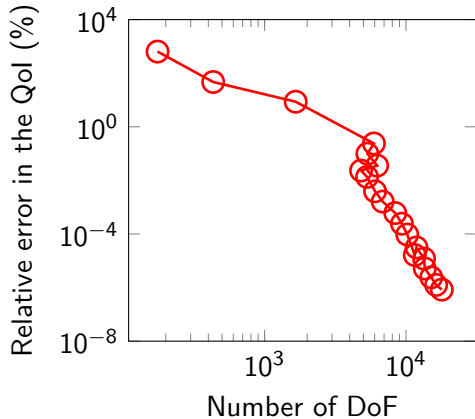
(b) Evolution of the relative error

Figure: Adaptive process for a Helmholtz problem

Illustrating the Goal-Oriented *hp*-Adaptivity



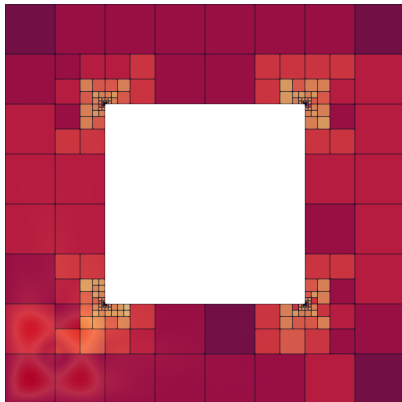
(a) Adaptive iteration 19 of 21



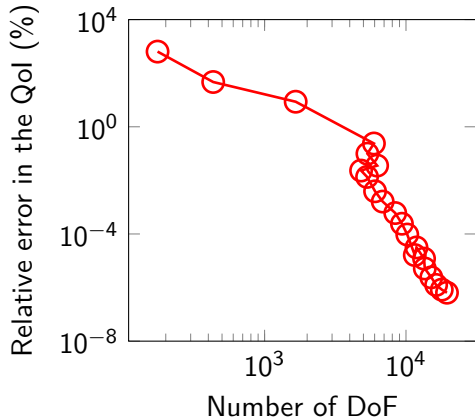
(b) Evolution of the relative error

Figure: Adaptive process for a Helmholtz problem

Illustrating the Goal-Oriented *hp*-Adaptivity



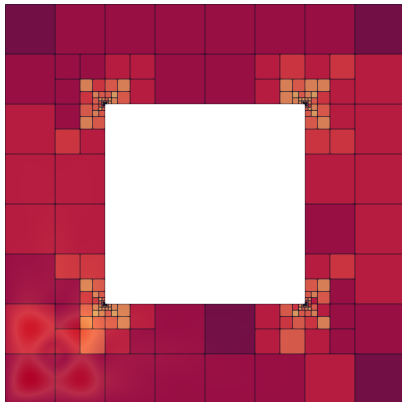
(a) Adaptive iteration 20 of 21



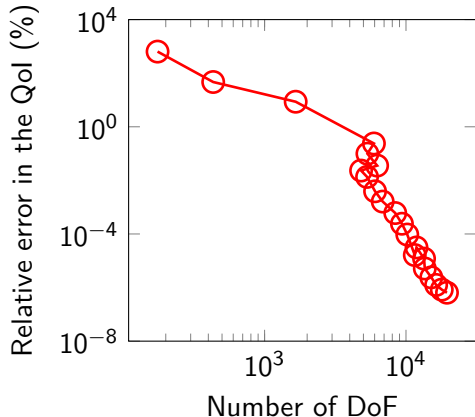
(b) Evolution of the relative error

Figure: Adaptive process for a Helmholtz problem

Illustrating the Goal-Oriented *hp*-Adaptivity



(a) Adaptive iteration 21 of 21



(b) Evolution of the relative error

Figure: Adaptive process for a Helmholtz problem

Main Ingredients

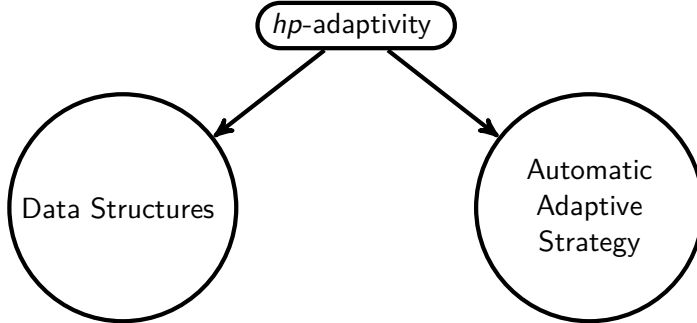


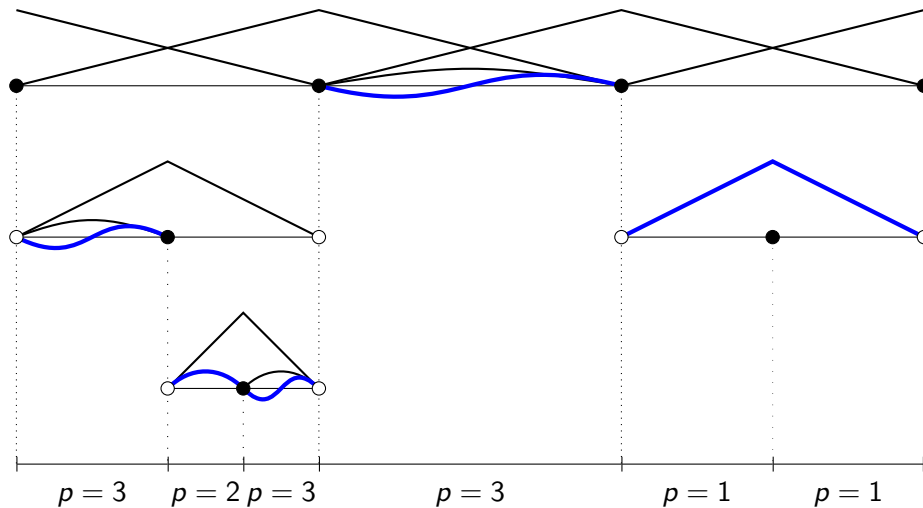
Figure: Main ingredients

Multi-Level Mesh Data Structure 1D

○ Dirichlet nodes

● Active nodes

— Basis functions



$p = 3$

$p = 2$ $p = 3$

$p = 3$

$p = 1$

$p = 1$

Multi-Level Mesh Data Structure 2D

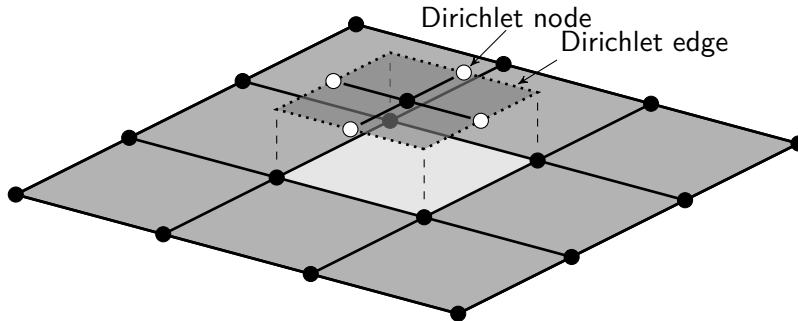


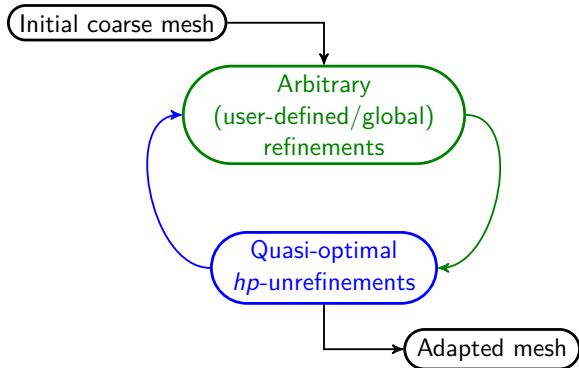
Figure: Multi-level 2D mesh without constraints on hanging nodes using Dirichlet nodes. The bubble basis functions are at the lowest level of each family



N. Zander, T. Bog, S. Kollmannsberger, D. Schillinger, and E. Rank

Multi-level *hp*-adaptivity: high-order mesh adaptivity without the difficulties of constraining hanging nodes
Computational Mechanics, 55(3):499–517, Mar 2015

A Painless Automatic Adaptive Strategy



V. Darrigrand, D. Pardo, T. Chaumont-Frelet, I. Gómez-Revuelto, L. E. García-Castillo

A painless automatic *hp*-adaptive strategy for elliptic problems

Finite Elements in Analysis and Design, 2020.



F. V. Caro, V. Darrigrand, J. Alvarez-Aramberri, E. Alberdi, D. Pardo

A painless multi-level automatic goal-oriented *hp*-adaptive coarsening strategy for elliptic and non-elliptic problems

Computer Methods in Applied Mechanics and Engineering, 2022.

Quasi-optimal hp -unrefinements

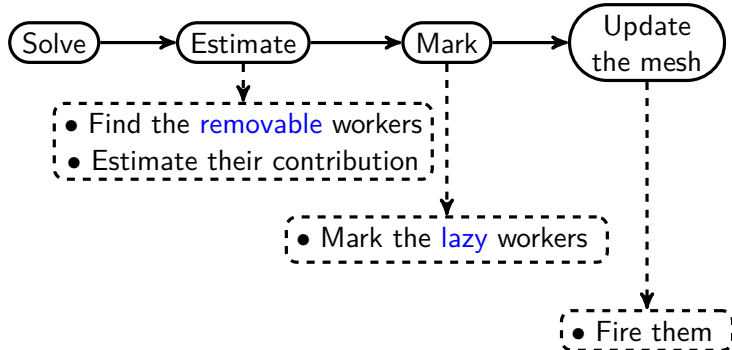
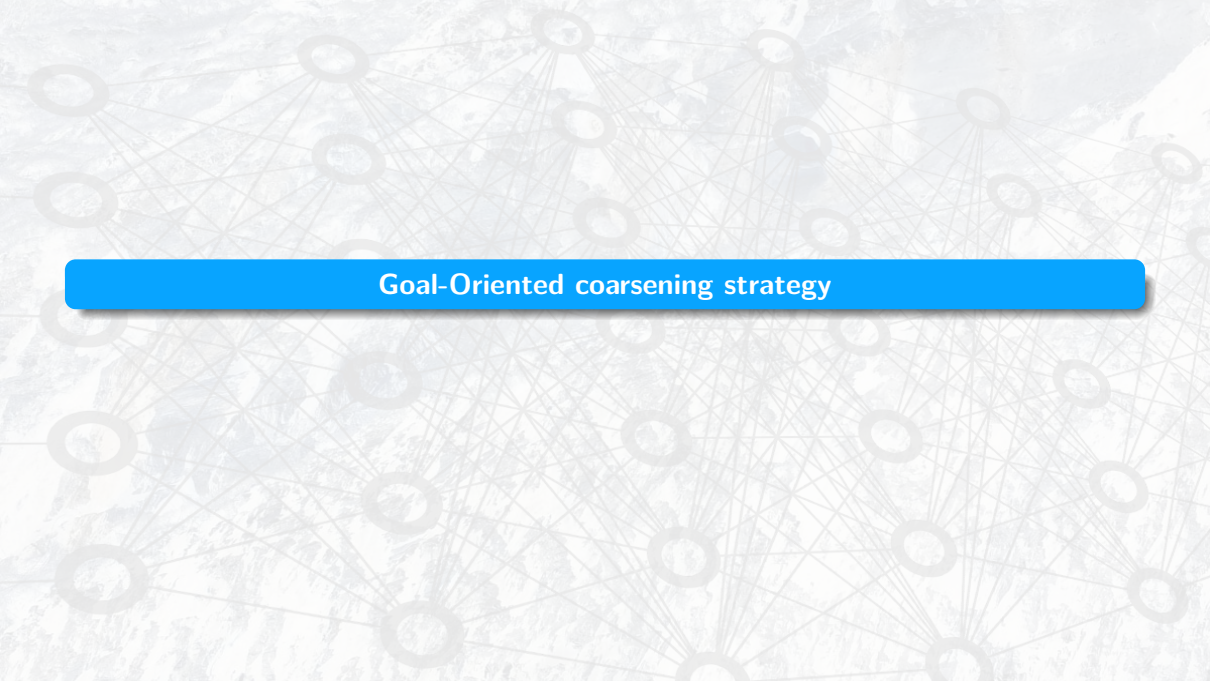


Figure: Quasi-optimal hp -unrefinement steps



Goal-Oriented coarsening strategy

Abstract Variational Formulation

Find $u_{\mathcal{F}} \in \mathbb{H}_{\mathcal{F}} \subset \mathbb{H}$ such that

$$b(u_{\mathcal{F}}, \phi_{\mathcal{F}}) = f(\phi_{\mathcal{F}}), \quad \forall \phi_{\mathcal{F}} \in \mathbb{H}_{\mathcal{F}}, \quad (1)$$

where:

- $f(\cdot)$ is a linear form defined on \mathbb{H} ,
- b is a bilinear form defined on $\mathbb{H} \times \mathbb{H}$,
- $\mathbb{H}_{\mathcal{F}} := \text{span}\{\phi_1, \dots, \phi_{n_{\mathcal{F}}}\}$ denotes the finite element space,
- $\mathcal{F} = \{\phi_i\}_{i=1}^{n_{\mathcal{F}}}$ is the set of basis functions defining $\mathbb{H}_{\mathcal{F}}$,
- $n_{\mathcal{F}}$ is the dimension of $\mathbb{H}_{\mathcal{F}}$, i.e., $n_{\mathcal{F}} = \dim(\mathbb{H}_{\mathcal{F}})$,
- $u_{\mathcal{F}}$ is the Galerkin approximation of u within $\mathbb{H}_{\mathcal{F}}$.

Projection Operator

Definition

Let $u_{\mathcal{F}}$ be the Galerkin approximation of u within $\mathbb{H}_{\mathcal{F}} \subset \mathbb{H}$ as follows:

$$u_{\mathcal{F}} := \sum_{\phi_i \in \mathcal{F}} u_i \phi_i, \quad (2)$$

where u_i are the coefficients corresponding to the basis functions ϕ_i in the set \mathcal{F} .

Definition of the Projection Operator

For a given subset of basis functions $\mathcal{S} \subset \mathcal{F}$ that generates the space $\mathbb{H}_{\mathcal{S}} \subset \mathbb{H}_{\mathcal{F}}$, we define our *projection operator* $\Pi_{\mathcal{F}}^{\mathcal{S}}: \mathbb{H}_{\mathcal{F}} \rightarrow \mathbb{H}_{\mathcal{S}}$ as

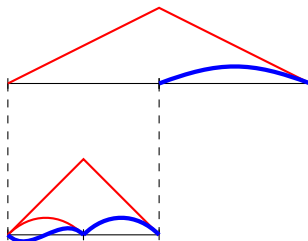
$$\Pi_{\mathcal{F}}^{\mathcal{S}} u_{\mathcal{F}} := \sum_{\phi_i \in \mathcal{S}} u_i \phi_i, \quad (3)$$

where we extract the coefficients of $u_{\mathcal{F}}$ corresponding to the basis functions in \mathcal{S} , and we set the others to zero.

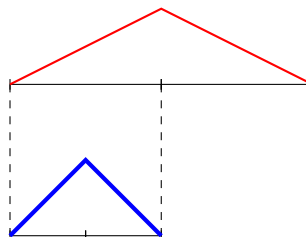
Removable 1D Basis Functions

Definition

We define **removable** basis functions as those we can eliminate from the discretization without modifying any other basis function while preserving **complete** polynomial spaces.



(a) *hp*-case



(b) *h*-case

Figure: Removable 1D basis functions

Basis Function Decomposition

Decomposition into Essential and Removable Basis Functions

- For any element K , consider:
 - \mathcal{R}_K : removable basis functions with support in K (cardinality $|\mathcal{R}_K|$).
 - $\mathbb{H}_{\mathcal{R}_K}$: space generated by \mathcal{R}_K .
 - $\mathcal{E}_K = \mathcal{F} \setminus \mathcal{R}_K$: essential basis functions.
 - $\mathbb{H}_{\mathcal{E}_K}$: space associated with \mathcal{E}_K .

Properties:

- $\mathbb{H}_{\mathcal{E}_K} \subset \mathbb{H}_{\mathcal{F}}$, $\mathbb{H}_{\mathcal{R}_K} \subset \mathbb{H}_{\mathcal{F}}$.
- $\mathbb{H}_{\mathcal{F}} = \mathbb{H}_{\mathcal{E}_K} \cup \mathbb{H}_{\mathcal{R}_K}$, $\mathbb{H}_{\mathcal{E}_K} \cap \mathbb{H}_{\mathcal{R}_K} = \emptyset$.

Hence, any function $u_{\mathcal{F}} \in \mathbb{H}_{\mathcal{F}}$ can be decomposed as:

$$u_{\mathcal{F}} = \Pi_{\mathcal{F}}^{\mathcal{E}_K} u_{\mathcal{F}} + \Pi_{\mathcal{F}}^{\mathcal{R}_K} u_{\mathcal{F}}. \quad (4)$$

Note: Projection of $u_{\mathcal{F}}$ onto \mathcal{E}_K approximates $u_{\mathcal{E}_K}$.

Error indicators in our Strategy

Let $\|\cdot\|_e$ be the *energy norm* associated with the Hilbert space \mathbb{H} .

For Elliptic Problems: The energy norm is defined from the bilinear form of the problem b as:

$$\|\cdot\|_e^2 = b(\cdot, \cdot).$$

For Non-Elliptic Problems: We define an alternative symmetric and positive definite operator a , not necessarily the original bilinear form, such that

$$|b(\phi, \psi)| \leq |a(\phi, \psi)|, \forall \phi, \psi \in \mathbb{H}$$

and the energy norm is

$$\|\cdot\|_e^2 = a(\cdot, \cdot).$$

The choice of these operators might highly influence the results of the adaptive process.

The Adjoint Problem

Find $v_{\mathcal{F}} \in \mathbb{H}_{\mathcal{F}} \subset \mathbb{H}$ such that

$$b(\phi_{\mathcal{F}}, v_{\mathcal{F}}) = I(\phi_{\mathcal{F}}), \quad \forall \phi_{\mathcal{F}} \in \mathbb{H}_{\mathcal{F}}, \quad (5)$$

where:

- the objective is to produce a space $\mathbb{H}_{\mathcal{F}}$ with minimal dimension such that the error in the Quantity of Interest (QoI) is below a user-defined tolerance,
- the QoI of the solution $u_{\mathcal{F}}$ is expressed as $I(u_{\mathcal{F}})$,
- $v_{\mathcal{F}}$ is the Galerkin approximation of v within $\mathbb{H}_{\mathcal{F}}$,
- $v_{\mathcal{E}_K}$ in \mathcal{E}_K is considered for analysis purposes, but not computed in practice.

Quantifying Changes in the Quantity of Interest (QoI)

For a given element $K \in \mathcal{T}$, we control

$$|I(u_{\mathcal{F}}) - I(u_{\mathcal{E}_K})|, \quad \forall K \in \mathcal{T},$$

where \mathcal{T} represents the discretization of \mathbb{H} into finite elements with $\mathbb{H}_{\mathcal{F}}$.

Using Galerkin Orthogonality: Since $\mathbb{H}_{\mathcal{E}_K} \subset \mathbb{H}_{\mathcal{F}}$, we have

$$b(u_{\mathcal{F}} - u_{\mathcal{E}_K}, \phi) = 0, \quad \forall \phi \in \mathbb{H}_{\mathcal{E}_K}. \quad (6)$$

Using Decomposition on $v_{\mathcal{F}}$:

$$I(u_{\mathcal{F}}) - I(u_{\mathcal{E}_K}) = b(u_{\mathcal{F}} - u_{\mathcal{E}_K}, v_{\mathcal{F}} - v_{\mathcal{E}_K}), \quad (7)$$

$$= b(u_{\mathcal{F}} - u_{\mathcal{E}_K}, \Pi_{\mathcal{F}}^{\mathcal{R}_K} v_{\mathcal{F}}). \quad (8)$$

Applying Decomposition and Orthogonality:

$$|I(u_{\mathcal{F}}) - I(u_{\mathcal{E}_K})| \simeq \left| b(\Pi_{\mathcal{F}}^{\mathcal{R}_K} u_{\mathcal{F}}, \Pi_{\mathcal{F}}^{\mathcal{R}_K} v_{\mathcal{F}}) \right| \leq \left| a(\Pi_{\mathcal{F}}^{\mathcal{R}_K} u_{\mathcal{F}}, \Pi_{\mathcal{F}}^{\mathcal{R}_K} v_{\mathcal{F}}) \right|. \quad (9)$$

Defining Element-wise Indicators:

$$\eta_K := \left| a(\Pi_{\mathcal{F}}^{\mathcal{R}_K} u_{\mathcal{F}}, \Pi_{\mathcal{F}}^{\mathcal{R}_K} v_{\mathcal{F}}) \right|, \quad \forall K \in \mathcal{T}. \quad (10)$$

1D Numerical results for Goal-Oriented h - and p -adaptivity

1D Numerical results for Goal-Oriented h - and p -adaptivity

Relative Error

The relative error in the QoI is:

$$e_{\text{rel}}^{\text{QoI}} := \frac{|I(u) - I(u_{\mathcal{T}_c})|}{|I(u)|} \times 100, \quad (11)$$

where u is the fine grid solution, $u_{\mathcal{T}_c}$ is the coarser mesh solution.

Helmholtz Goal-Oriented problem

Find u such that:

$$-u'' - k^2 u = \mathbf{1}_{(0, \frac{2}{5})} \quad \text{in } (0, 1), \quad (12)$$

$$u(0) = 0, \quad (13)$$

$$u'(1) = 0. \quad (14)$$

QoI: $I(u) = 5 \int_{\frac{3}{5}}^{\frac{4}{5}} u \, dx$. The operator $a(\cdot, \cdot)$ is the 1D Laplace operator.

Solution and Final Adaptive Meshes

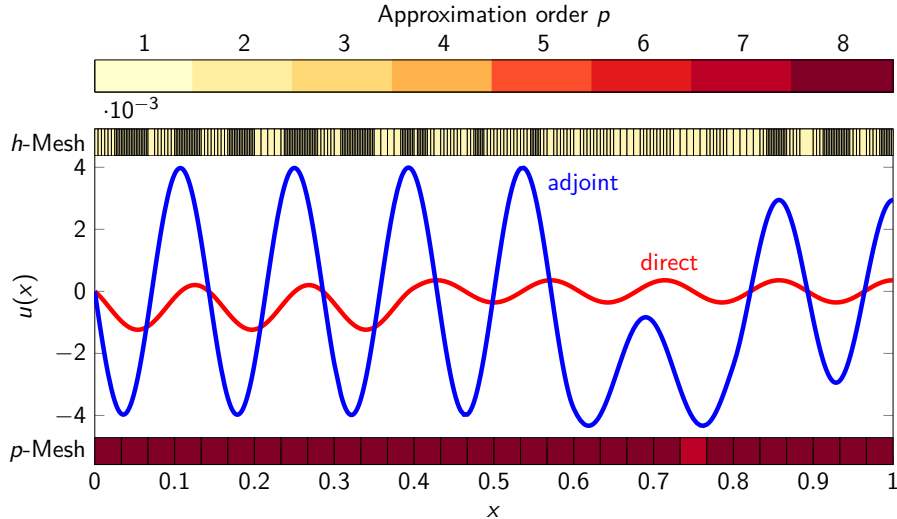


Figure: Solutions with $k = 7 \cdot 2\pi$ problem after the h -adaptive process.

Evolution of the Relative Error: h -adaptivity

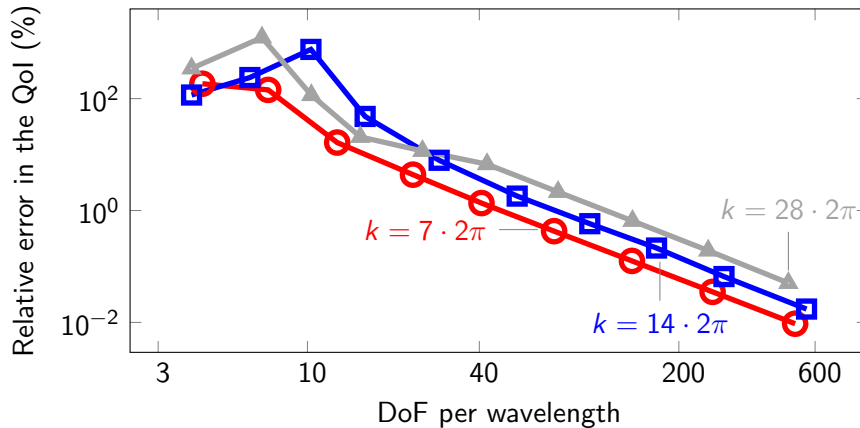


Figure: Evolution of $e_{\text{rel}}^{\text{QoI}}$ using h -adaptivity. Initial mesh size $h = \frac{1}{30}$ and uniform $p = 1$.

Evolution of the Relative Error: p -adaptivity

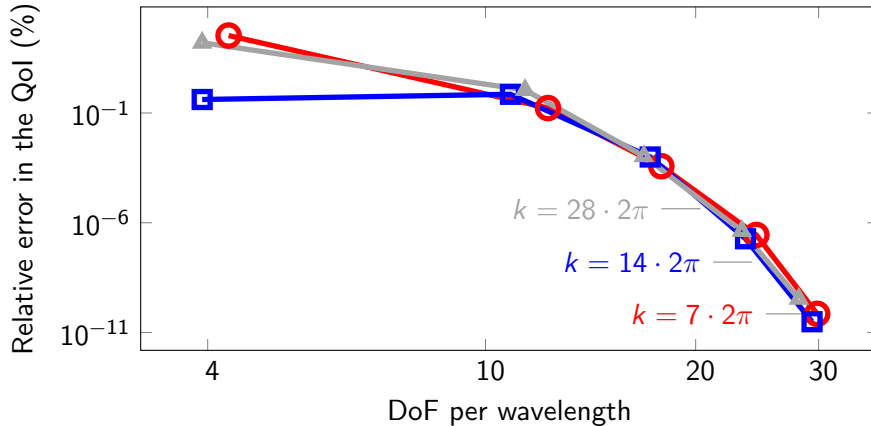


Figure: Evolution of $e_{\text{rel}}^{\text{QoI}}$ using p -adaptivity. Uniform mesh size $h = \frac{1}{30}$.

2D Numerical results for hp -adaptivity

2D Numerical results for hp -adaptivity

The relative error

In energy-norm adaptivity, we define the relative error in percentage as:

$$\tilde{e}_{\text{rel}}^{\text{energy}} := \frac{\|u - u_{\mathcal{T}_c}\|_{\mathbb{H}}}{\|u\|_{\mathbb{H}}} \cdot 100. \quad (15)$$

Our Quantity of Interest (QoI)

For the GOA problems, we define our QoI as

$$I(\phi) = \frac{1}{|\Omega_I|} \langle \mathbb{1}_{\Omega_I}, \phi \rangle_{L^2(\Omega)}, \quad \forall \phi \in \mathbb{H}, \quad (16)$$

where:

- $|\Omega_I|$ defines the area or volume of Ω_I ,
- $\mathbb{1}_{\Omega_I}$ is a function equal to one if $x \in \Omega_I$, and zero otherwise.

2D Numerical results for hp -adaptivity

Wave propagation problem

Find u satisfying:

$$-\Delta u - k^2 u = \mathbb{1}_{\Omega_f} \quad \text{in } \Omega, \tag{17}$$

$$u = 0 \quad \text{on } \Gamma_D, \tag{18}$$

$$\nabla u \cdot \vec{n} = 0 \quad \text{on } \Gamma_N. \tag{19}$$

Domain Definitions:

- $\Omega_f = \left(0, \frac{1}{4}\right)^2 \subset \Omega$,
- $k = (8 \cdot 2\pi, 2\pi)$,
- $\Omega_I = \left(\frac{3}{4}, 1\right)^2 \subset \Omega$,
- $a(\cdot, \cdot) :=$

$$\left| \langle \nabla \cdot, \nabla \cdot \rangle_{L^2(\Omega)} \right| + |k^2| \left| \langle \cdot, \cdot \rangle_{L^2(\Omega)} \right|.$$

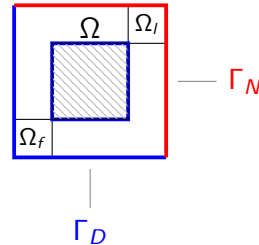
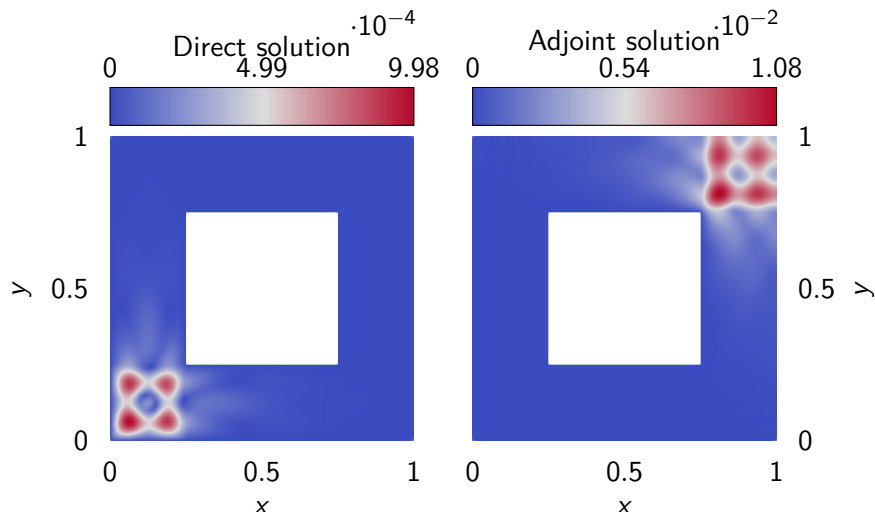
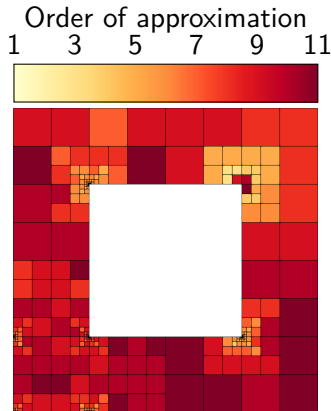


Figure: Domain $\Omega = (0, 1)^2 \setminus (\frac{1}{4}, \frac{3}{4})^2 \subset \mathbb{R}^2$.

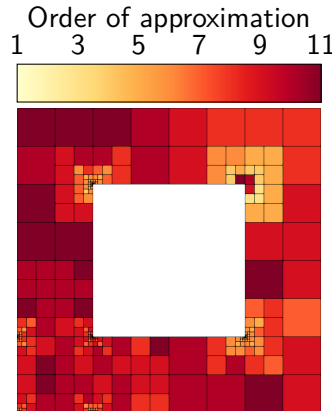
Wave propagation problem



Energy-norm adaptivity

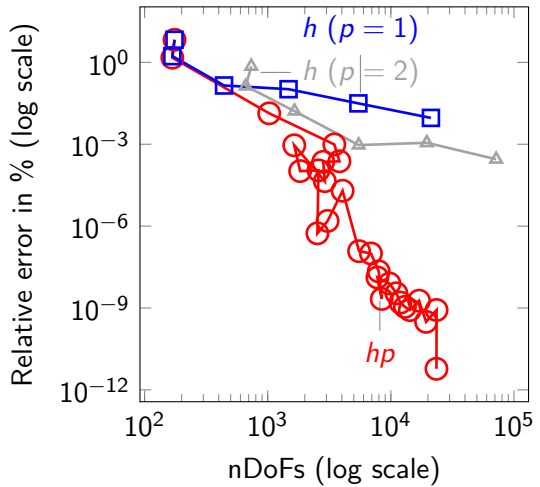


(a) Final hp -adapted mesh with polynomial orders in the x-direction.

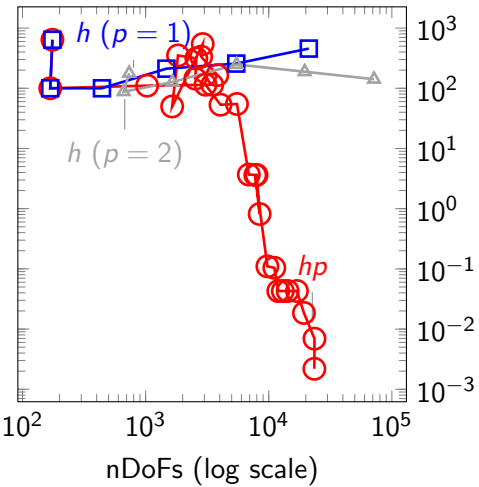


(b) Final hp -adapted mesh with polynomial orders in the y-direction.

Energy-norm adaptivity

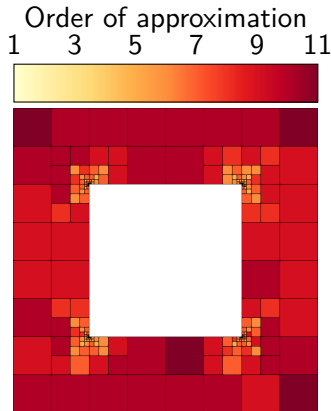


(a) Evolution of $\tilde{e}_{\text{rel}}^{\text{energy}}$ in the process.

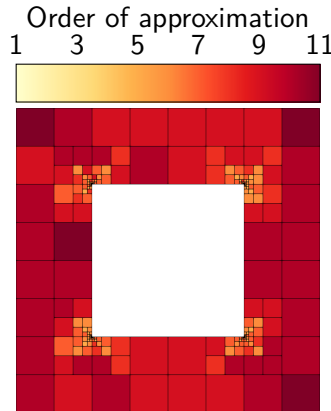


(b) Evolution of $e_{\text{rel}}^{\text{QoI}}$ in the process.

Goal-Oriented adaptivity

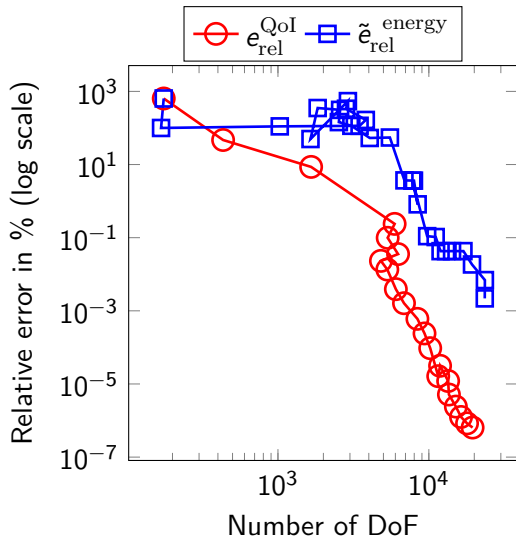


(a) Final hp -adapted mesh with polynomial orders in the x-direction.

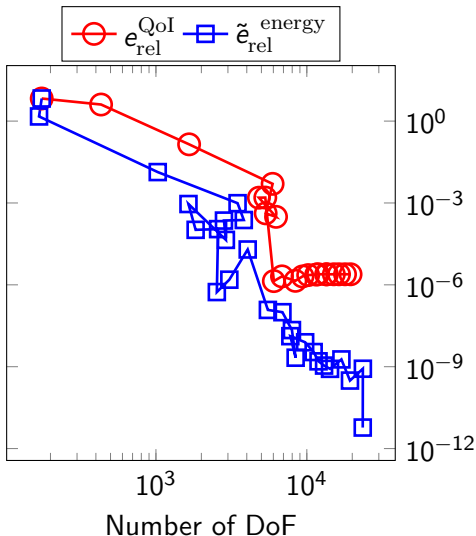


(b) Final hp -adapted mesh with polynomial orders in the y-direction.

Energy-norm and Goal-Oriented hp -adaptive strategies



(a) Evolution of goal-oriented adaptivity.



(b) Evolution of energy-norm adaptivity.

Goal-Oriented hp -adaptivity for parametric PDEs

A Goal-Oriented strategy for parametric PDEs

Definitions

- Let \mathbf{m}_i denote a collection of P parameters: $\mathbf{m}_i = \{\sigma_1, \dots, \sigma_P\}$.
- Let $\mathbf{M} = \{\mathbf{m}_1, \dots, \mathbf{m}_S\}$ be a set of S samples.

σ_1^1	σ_2^1
σ_3^1	σ_4^1

\mathbf{m}_1

σ_1^2	σ_2^2
σ_3^2	σ_4^2

\mathbf{m}_2

σ_1^S	σ_2^S
σ_3^S	σ_4^S

...

\mathbf{m}_S

Figure: Representation of S different samples.

Abstract Variational Formulation

Find $u_{\mathcal{F}}^{\mathbf{m}} \in \mathbb{H}_{\mathcal{F}}$ such that

$$b^{\mathbf{m}}(u_{\mathcal{F}}^{\mathbf{m}}, \phi_{\mathcal{F}}) = f^{\mathbf{m}}(\phi_{\mathcal{F}}), \quad \forall \phi_{\mathcal{F}} \in \mathbb{H}_{\mathcal{F}}, \quad (20)$$

where:

- $b^{\mathbf{m}}$ corresponds to the bilinear form that characterizes the problem related to the model \mathbf{m} ,
- $f^{\mathbf{m}}(\cdot)$ is a linear form.

Find $v_{\mathcal{F}}^{\mathbf{m}} \in \mathbb{H}_{\mathcal{F}}$ such that

$$b^{\mathbf{m}}(\phi_{\mathcal{F}}, v_{\mathcal{F}}^{\mathbf{m}}) = l^{\mathbf{m}}(\phi_{\mathcal{F}}), \quad \forall \phi_{\mathcal{F}} \in \mathbb{H}_{\mathcal{F}}, \quad (21)$$

where:

- $l^{\mathbf{m}}(\cdot)$ is a linear continuous form.

A Goal-Oriented strategy for parametric PDEs

Objective

We are interested in controlling $|I(u_{\mathcal{F}}^{\mathbf{m}}) - I(u_{\mathcal{E}_K}^{\mathbf{m}})|, \forall K \in \mathcal{T}$.

Approximation and Bound

We find that:

$$|I(u_{\mathcal{F}}^{\mathbf{m}}) - I(u_{\mathcal{E}_K}^{\mathbf{m}})| \simeq |b(\Pi_{\mathcal{F}}^{\mathcal{R}_K} u_{\mathcal{F}}^{\mathbf{m}}, \Pi_{\mathcal{F}}^{\mathcal{R}_K} v_{\mathcal{F}}^{\mathbf{m}})| \leq |a(\Pi_{\mathcal{F}}^{\mathcal{R}_K} u_{\mathcal{F}}^{\mathbf{m}}, \Pi_{\mathcal{F}}^{\mathcal{R}_K} v_{\mathcal{F}}^{\mathbf{m}})|, \quad (22)$$

where a is an alternative operator —not necessarily the original bilinear form.

Isotropic Element-wise Indicators

Therefore, we define the isotropic element-wise indicators $\eta_K, \forall K \in \mathcal{T}$, as:

$$\eta_K^{\mathbf{m}} := |a(\Pi_{\mathcal{F}}^{\mathcal{R}_K} u_{\mathcal{F}}^{\mathbf{m}}, \Pi_{\mathcal{F}}^{\mathcal{R}_K} v_{\mathcal{F}}^{\mathbf{m}})|, \quad \forall K \in \mathcal{T}. \quad (23)$$

MAGO: (M)ulti-(A)daptive (G)oal-(O)riented

Abstract Variational Formulation

Find $u_{\mathcal{F}}^{\mathbf{m}_i} \in \mathbb{H}_{\mathcal{F}}$ such that

$$b^{\mathbf{m}_i}(u_{\mathcal{F}}^{\mathbf{m}_i}, \phi_{\mathcal{F}}) = f^{\mathbf{m}_i}(\phi_{\mathcal{F}}), \quad \forall \phi_{\mathcal{F}} \in \mathbb{H}_{\mathcal{F}}. \quad (24)$$

Find $v_{\mathcal{F}}^{\mathbf{m}_i} \in \mathbb{H}_{\mathcal{F}}$ such that

$$b^{\mathbf{m}_i}(\phi_{\mathcal{F}}, v_{\mathcal{F}}^{\mathbf{m}_i}) = l^{\mathbf{m}_i}(\phi_{\mathcal{F}}), \quad \forall \phi_{\mathcal{F}} \in \mathbb{H}_{\mathcal{F}}. \quad (25)$$

where $i = 1, \dots, S$, indicating that we solve S forward and adjoint discrete problems.

Objective

Build a single final hp -mesh, optimizing its size to be as small as possible for all the samples in a single GOA process.

MAGO: (M)ulti-(A)daptive (G)oal-(O)riented

Termination Criterion

To control the relative error the QoI, ensuring that it falls within a specified tolerance TOL :

$$\max_{i, \{\mathbf{m}_i\}_{i=1}^S} \left\{ \frac{|I(u^{\mathbf{m}_i}) - I(u_{T_c}^{\mathbf{m}_i})|}{|I(u^{\mathbf{m}_i})|} \right\} < TOL. \quad (26)$$

Coarsening Step with a Single Mesh

We employ a coarsening step using a single mesh, which involves the following stages:

- ① Solve the finite element method (FEM) problem for each \mathbf{m}_i .
- ② Compute element-wise error indicators for each \mathbf{m}_i .
- ③ Combine all the element-wise error indicators into a unified measure.
- ④ Perform mesh unrefinement based on the combined error measure.

MAGO: (M)ulti-(A)daptive (G)oal-(O)riented

η_1^1	η_2^1	η_3^1	η_4^1
η_5^1	η_6^1	η_7^1	η_8^1
η_9^1	η_{10}^1	η_{11}^1	η_{12}^1
η_{13}^1	η_{14}^1	η_{15}^1	η_{16}^1

\mathbf{m}_1

η_1^2	η_2^2	η_3^2	η_4^2
η_5^2	η_6^2	η_7^2	η_8^2
η_9^2	η_{10}^2	η_{11}^2	η_{12}^2
η_{13}^2	η_{14}^2	η_{15}^2	η_{16}^2

\mathbf{m}_2

η_1^S	η_2^S	η_3^S	η_4^S
η_5^S	η_6^S	η_7^S	η_8^S
η_9^S	η_{10}^S	η_{11}^S	η_{12}^S
η_{13}^S	η_{14}^S	η_{15}^S	η_{16}^S

...

\mathbf{m}_S

A single *hp*-grid →

η_1	η_2	η_3	η_4
η_5	η_6	η_7	η_8
η_9	η_{10}	η_{11}	η_{12}
η_{13}	η_{14}	η_{15}	η_{16}

Different Alternatives
to combine the
error indicators:

l_1 -norm, l_2 -norm, l_∞ -norm

Numerical results

Wave propagation problem

Find u satisfying:

$$-\nabla \cdot (\nabla u) - j\sigma(\mathbf{x}) u = 1 \text{ in } \Omega, \quad (27)$$

$$u = 0 \text{ on } \partial\Omega. \quad (28)$$

Domain Definitions:

- $\Omega_f = \left(\frac{1}{20}, \frac{3}{20}\right)^2,$
- $\Omega_I = \left(\frac{17}{20}, \frac{19}{20}\right)^2,$
- $\Omega = (0, 1)^2 \subset \mathbb{R}^2.$

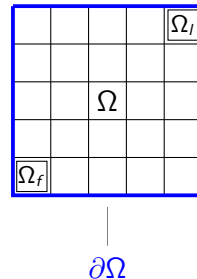
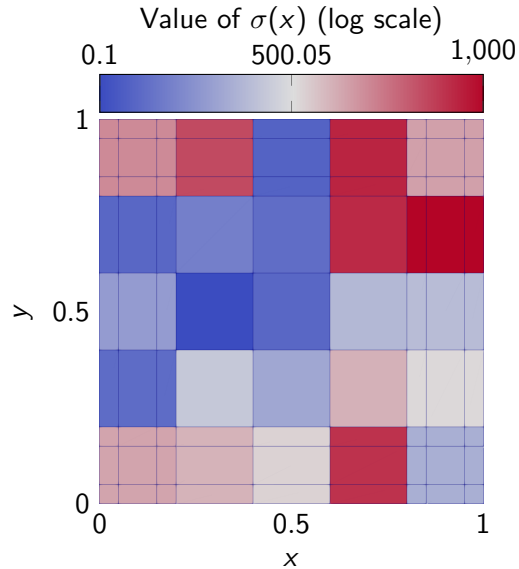
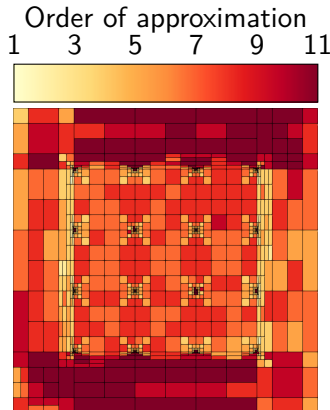


Figure: Domain illustration (5×5 grid).

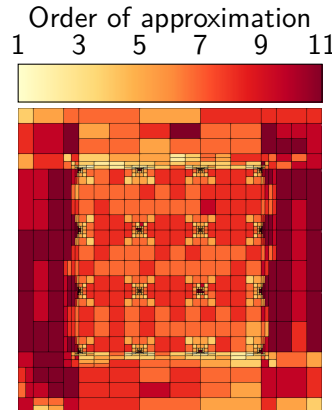
Values for the materials in the domain



Final MAGO *hp*-adapted meshes



(a) Final *hp*-adapted mesh with polynomial orders in the x-direction.



(b) Final *hp*-adapted mesh with polynomial orders in the y-direction.

Contrasting Norms in Error Indicators

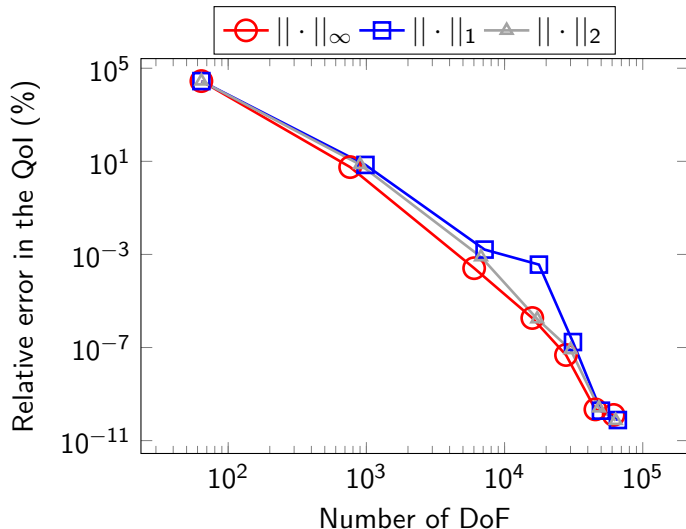


Figure: Convergence for different norms in the error indicators (100 samples)

MAGO: Testing the Adaptive Meshes with 10K Samples

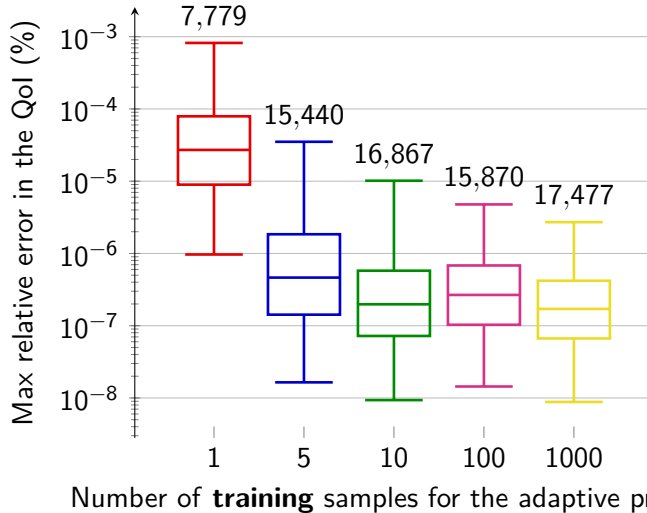


Figure: Different adaptive grids with a threshold maximum relative error set at 10^{-5} .

Computational costs of generating the database

Computational cost C^{SAGO}

For dimension $d = 2$, we approximate the computational cost C^{SAGO} of generating one GOA mesh for each of the S_G samples by:

$$C^{\text{SAGO}} \approx \sum_{i=1}^{S_G} \left(N_{f(i)}^{\text{sago}} \right)^{\left(1 + \frac{d-1}{2}\right)}. \quad (29)$$

Computational cost C^{MAGO}

In addition, we provide an approximate estimation of the computational costs for MAGO by:

$$C^{\text{MAGO}} \approx \sum_{i=1}^{S_A} \left(N_{f(i)}^{\text{mago}} \right)^{\left(1 + \frac{d-1}{2}\right)} + \sum_{i=1}^{S_G} \left(N_{c(i)}^{\text{mago}} \right)^{\left(1 + \frac{d-1}{2}\right)}. \quad (30)$$

Computational Costs: SAGO vs. MAGO Strategies

Number of DoF		C^{SAGO}			
		S_G			
N_f^{sago}		10^5	10^7	10^9	10^{11}
41259		$8.4 \cdot 10^{11}$	$8.4 \cdot 10^{13}$	$8.4 \cdot 10^{15}$	$8.4 \cdot 10^{17}$

Number of DoF		C^{MAGO}				
		S_G				
S_A	N_c^{mago}	N_f^{mago}	10^5	10^7	10^9	10^{11}
5	15440	52351	$1.9 \cdot 10^{11}$	$1.9 \cdot 10^{13}$	$1.9 \cdot 10^{15}$	$1.9 \cdot 10^{17}$
10	16867	57171	$2.2 \cdot 10^{11}$	$2.2 \cdot 10^{13}$	$2.2 \cdot 10^{15}$	$2.2 \cdot 10^{17}$
100	15870	53661	$2.0 \cdot 10^{11}$	$2.0 \cdot 10^{13}$	$2.0 \cdot 10^{15}$	$2.0 \cdot 10^{17}$
1000	17477	60381	$2.5 \cdot 10^{11}$	$2.3 \cdot 10^{13}$	$2.3 \cdot 10^{15}$	$2.3 \cdot 10^{17}$

Main Achievements

Main Achievements

Peer-Reviewed Publications

-  F. V. Caro, V. Darrigrand, J. Alvarez-Aramberri, and D. Pardo. "A Multi-Adaptive-Goal-Oriented Strategy to Generate Massive Databases of Parametric PDEs," To be submitted to *Computer Methods in Applied Mechanics and Engineering*, December 2023.
-  F. V. Caro, V. Darrigrand, J. Alvarez-Aramberri, E. Alberdi, and D. Pardo. "A Painless Multi-Level Automatic Goal-Oriented hp -Adaptive Coarsening Strategy for Elliptic and Non-Elliptic Problems," *Computer Methods in Applied Mechanics and Engineering*, vol. 401, 115641, 2022. <https://doi.org/10.1016/j.cma.2022.115641>
-  F. V. Caro, V. Darrigrand, J. Alvarez-Aramberri, E. A. Celaya, and D. Pardo. "1D Painless Multi-Level Automatic Goal-Oriented h and p Adaptive Strategies Using a Pseudo-Dual Operator," In *Computational Science – ICCS 2022*, pp. 347–357, 2022.
https://doi.org/10.1007/978-3-031-08754-7_43

Main Achievements

Conference Talks

- [1] F. V. Caro, V. Darrigrand, J. Alvarez-Aramberri, and D. Pardo.
Databases for Deep Learning Inversion Using A Goal-Oriented hp-Adaptive Strategy.
XI International Conference on Adaptive Modeling and Simulation,
Gothenburg, Sweden, June 19-21, 2023.
- [2] F. V. Caro, V. Darrigrand, J. Alvarez-Aramberri, E. Alberdi, and D. Pardo.
*A Painless Automatic hp-Adaptive Coarsening Strategy For Non-SPD problems:
A Goal-Oriented Approach.* 15th World Congress on Computational Mechanics
& 8th Asian Pacific Congress on Computational Mechanics,
Yokohama, Japan, July 31 - August 5, 2022.
- [3] F. V. Caro, V. Darrigrand, J. Alvarez-Aramberri, E. Alberdi, and D. Pardo.
*1D Painless Multi-Level Automatic Goal-Oriented h and p Adaptive Strategies using
a Pseudo-Dual Operator.* 22nd International Conference on Computational Science,
London, United Kingdom, June 21-23, 2022.

Main Achievements

Conference Talks

- [4] F. V. Caro, V. Darrigrand, J. Alvarez-Aramberri, E. Alberdi, and D. Pardo.
Goal-Oriented hp-Adaptive Finite Element Methods: A Painless Multilevel Automatic Coarsening Strategy For Non-SPD Problems. 8th European Congress on Computational Methods in Applied Sciences and Engineering, Oslo, Norway, June 5-9, 2022.
- [5] F. V. Caro, V. Darrigrand, J. Alvarez-Aramberri, E. Alberdi, and D. Pardo.
A Painless Goal-Oriented hp-Adaptive Strategy for Indefinite Problems.
16th U.S. National Congress on Computational Mechanics,
Chicago, U.S.A, July 25-29, 2021.
- [6] F. V. Caro, V. Darrigrand, J. Alvarez-Aramberri, E. Alberdi, and D. Pardo.
Goal-Oriented hp-Adaptive Finite Element Methods: A Painless Multi-level Automatic Coarsening Strategy. 10th International Conference on Adaptive Modeling and Simulation, Gothenburg, Sweden, June 21-23, 2021.

Main Achievements

Research Stays

FEB. 2023 – MAR. 2023
(2 months) University of Science and Technology (AGH),
Krakow (Poland).

Supervisor: Maciej Paszynski.

SEP. 2021 – NOV. 2021
(2 months) CNRS-IRIT-ENSEEIHT (N7),
Toulouse (France).

Supervisor: Vincent Darrigrand.

NOV. 2020 – DEC. 2020
(1 month) CNRS-IRIT-ENSEEIHT (N7),
Toulouse (France).

Supervisor: Vincent Darrigrand.

Conclusions and Future Work

Contributions

- We have employed hierarchical basis functions that effectively address the challenge of *hanging nodes*.
- We have developed **simple-to-implement** h - and p -GOA strategies that use an unconventional symmetric and positive definite bilinear form for possibly non-elliptic goal-oriented problems.
- We have expanded upon a painless automatic hp strategy, initially developed for energy-norm adaptivity, to both non-elliptic and goal-oriented problems.
- We have extended the applicability of a coarsening strategy to encompass parametric PDEs.

Future Work

- Extend algorithms to address multi-physics problems, notably $H(\text{curl})$ and $H(\text{div})$.
- Validate the efficacy of our algorithms in real-world scenarios such as Magnetotellurics, Controlled Sources, and Logging While Drilling.
- Analyze the impact of the nature and distribution of various random samples on DL inversion for optimization.
- Enhance parallelization and factorization techniques to reduce computational resource requirements in future applications.

Research Stays

Bilbao



Toulouse



Kraków

